roscopic rheological parameters, such as viscosity and normal stress measured either for large (*3, 4*) or small (*5*) gaps. Our results show the crucial importance of a direct structural probe, such as synchrotron x-ray scattering, in the elucidation of the microstructure that underlies the macroscopic rheological shear and normal stress responses of flowing complex fluids.

REFERENCES AND NOTES

1. G. K. Batchelor, *An Introduction to Fluid Dynamics* (Cambridge Univ. Press, Cambridge, 1970).
2. See, for example, P. G. de Gennes, *Scaling Concepts in Polymer Physics* (Cornell Univ. Press, Ithaca, NY, 1979); S. A. Safran and N. A. Clark, Eds., *Physics of Complex and Supermolecular Fluids* (Wiley, New York, 1987); C. R. Safinya, S. A. Safran, P. A. Pincus, Eds., *Macromolecular Liquids*, vol. 177 of *Materials Research Society Symposium Proceedings* (Materials Research Society, Pittsburgh, PA, 1990).
3. K. Weissenberg, *Nature* **159**, 310 (1947).
4. P. Oswald and M. Kleman, *J. Phys.* (*Paris*) *Lett.* **43**, 411 (1982); T. E. Fischer, S. Bhattacharya, R. Salher, J. L. Lauer, Y.-J. Ahn, *Tribol. Trans.* **31**, 442 (1988).
5. J. N. Israelachvili, P. M. McGuiggan, A. M. Homola, *Science* **240**, 189 (1988); J. Van Alsten and S. Granick, *Phys. Rev. Lett.* **61**, 2570 (1988); J. Klein, D. Perahia, S. Warburg, *Nature* **352**, 143 (1991).
6. J. R. A. Pearson, in *Mechanics of Polymer Processing* (Elsevier, London, 1985).
7. J. D. Litster and R. J. Birgeneau, *Phys. Today* **35** (no. 5), 26 (1982); P. S. Pershan, *Structure of Liquid Crystal Phases* (World Scientific, Singapore, 1988); D. Davidov *et al.*, *Phys. Rev. B* **19**, 1657 (1979).
8. C. R. Safinya *et al.*, *Phys. Rev. Lett.* **57**, 2718 (1986); C. R. Safinya, E. B. Sirota, D. Roux, G. S. Smith, *ibid.* **62**, 1134 (1989); G. S. Smith, E. B. Sirota, C. R. Safinya, R. J. Plano, N. A. Clark, *J. Chem. Phys.* **92**, 4519 (1990); D. Roux, C. R. Safinya, F. Nallet, in *Modern Amphiphilic Physics*, A. Ben-Shaul, W. Gelbart, D. Roux, Eds. (Springer, New York, in press).
9. P. G. de Gennes, *The Physics of Liquid Crystals* (Oxford Univ. Press, London, 1974).
10. R. J. Plano, C. R. Safinya, E. B. Sirota, L. Wenzel, *Rev. Sci. Instrum.* **64**, 1309 (1993).
11. M. Miecowicz, *Nature* **158**, 27 (1946).
12. O. Diat and D. Roux, *J. Phys.* (*Paris*), in press.
13. R. G. Horn and M. Kleman, *Ann. Phys.* (*Paris*) **3**, 229 (1978); R. Ribotta and G. Durand, *J. Phys.* (*Paris*) **38**, 179 (1977).
14. In the high-shear regime, the elastic torque attributable to the spatial dependence of the director, because of textural defects or boundary conditions or both, can be neglected as described in (*9, 17*).
15. K. A. Koppi, M. Tirrell, F. S. Bates, K. Almdal, R. H. Colby, *J. Phys.* (Paris) **2**, 1941 (1992); K. A. Koppi, M. Tirrell, F. S. Bates, *Phys. Rev. Lett.* **70**, 1449 (1993).
16. C. R. Safinya, E. B. Sirota, R. Plano, R. Bruinsma, *J. Phys. Condens. Matter* **2**, SA365 (1990); C. R. Safinya, E. B. Sirota, R. Plano, *Phys. Rev. Lett.* **66**, 1986 (1991).
17. W. L. McMillan, *Phys. Rev. A* **9**, 1720 (1974); F. Janig and F. Brochard, *J. Phys.* (*Paris*) **35**, 301 (1974).
18. R. F. Bruinsma and C. R. Safinya, *Phys. Rev. A* **43**, 5377 (1991).
19. P. Pieranski and E. Guyon, *Phys. Rev. Lett.* **32**, 924 (1974); K. Skarp *et al.*, *Mol. Cryst. Liq. Cryst.* **66**, 199 (1981).
20. To fix $De = \gamma\tau$ for the numerical runs, we determined the fluctuation relaxation time $\tau = (2/\pi)(\alpha_3^R - \alpha_3)(\xi_\| d^2/k_B T)$ using the experimental data: (i) $\alpha_3^R/|\alpha_2| = (n_{\nabla v}/n_v)^2$, the ratio of the widths of the x-ray data measured in the nematic phase along the ∇v and v directions [described in (*16*)]; (ii) in 8CB, $|\alpha_2| \approx 3$ poise, independent of T (*19*); and (iii) the measured equilibrium value of $\xi_\|(t)$ for 8CB was used (*7*).
21. We note that for an arbitrary orientation of $\hat{n}$, the corresponding scattering spot points along $\hat{n}$ and occurs at $\mathbf{q} = q_0\hat{n}$ in reciprocal space. Thus, an anisotropic (isotropic) distribution of $\hat{n}$ about the z axis would result in a corresponding anisotropic (or isotropic) scattering "patch" on a sphere of radius q_0 centered about the q_z axis.
22. We gratefully acknowledge conversations with R. Larson, J. Prost, D. Roux, and, in particular, J. Israelachvili and T. Witten. Synchrotron x-ray scattering experiments carried out on beam line X-10A at the National Synchrotron Light Source at the Brookhaven National Laboratories, which is supported by the U.S. Department of Energy. The Materials Research Laboratory at Santa Barbara is supported by National Science Foundation grant DMR-9123048. Supported in part by Office of Naval Research grant N00014-93-1-0269 (C.R.S.).

6 April 1993; accepted 4 June 1993

Relation of Major Volcanic Center Concentration on Venus to Global Tectonic Patterns

L. S. Crumpler, James W. Head, Jayne C. Aubele

Global analysis of NASA Magellan image data indicates that a major concentration of volcanic centers covering ~40 percent of the surface of Venus occurs between the Beta, Atla, and Themis regiones. Associated with this enhanced concentration are geological characteristics commonly interpreted as rifting and mantle upwelling. Interconnected low plains in an annulus around this concentration are characterized by crustal shortening and infrequent volcanic centers that may represent sites of mantle return flow and net downwelling. Together, these observations suggest the existence of relatively simple, large-scale patterns of mantle circulation similar to those associated with concentrations of intraplate volcanism on Earth.

Detailed volcanological observations of the surface of Venus that are necessary to address fundamental questions about its geological comparisons with Earth are now possible with Magellan synthetic aperture and altimetry radar data (*1*). Here, we concentrate on the distribution of these volcanic centers, their correlation with global geological characteristics, and the possible origin of these global characteristics through large-scale mantle anomalies and dynamic patterns.

The initial analysis of Magellan data resulted in the identification, description, and location, to the nearest half-degree, of 1662 individual volcanic centers and related features larger than 20 km in diameter (*2–5*). On the basis of the resulting global distribution map (Fig. 1A), volcanic centers >20 km in diameter are not randomly distributed but are instead concentrated in certain specific regions. This pattern is in contrast to that for impact craters on Venus, the distribution of which cannot be distinguished from that expected for a completely spatially random case (*6*). However, volcanic centers are not arranged in linear patterns as are plate boundary volcanoes on Earth. In this respect and in terms of the estimated global volume flux (<1 km^3 per year) of associated volcanism (*2*), they are comparable to intraplate volcanism (hot spots) on Earth.

Department of Geological Sciences, Brown University, Providence, RI 02912.

Areas over which the concentration of volcanic centers exceeds the global mean density (3.5 ± 2.9 centers per 10^6 km^2) by at least 2σ vary in width from a few hundred to a few thousand kilometers in diameter over physiographically well defined areas (Fig. 1B). An equidimensional region ~13,000 km in diameter of moderate to high areal abundance of volcanic centers (>3 to 7 centers per 10^6 km^2) is centered near the equator at longitude ~250°E between the Beta, Atla, and Themis regiones (BAT). For comparison, the maximum density of hot spot volcanic centers on Earth (*7*) is ~0.1 to 0.2 centers per 10^6 km^2 (*8*). This smaller figure for Earth reflects the relatively younger age of Earth's sea floor (~70 million years) relative to the inferred average surface age (0.5 billion years) of Venus (*9*) and the greater number of volcanic features on Venus, many of which may not be of hot spot origin. Although the BAT anomaly is the largest global concentration, smaller concentrations with similar density occur clustered about the equator in the opposite hemisphere near longitude 70°E. Similar hemispherically symmetric distributions and hemispherically asymmetric concentration levels characterize the distribution of intraplate volcanic centers (hot spots) on Earth (*10*).

The area of the BAT anomaly covers up to ~40% of the global surface, and the density of the volcanic centers exceeds the global mean density over >50% of the surface of Venus. Volcanic centers occur with greatest frequency at intermediate altitudes ("uplands") between 1 and 2 km above the mean planetary radius. Consequently, the spatial density of volcanic centers is less than the mean in relatively well defined areas that primarily include lowlands [elevations ≤6051.84 km (mean radius)] and highlands (elevations >2 km above the mean radius). Lowland areas encircle the BAT anomaly and occur as elongate and interconnected plains oriented east-west in the mid-north or mid-south latitudes (Sedna, Aino, and Helen planitiae) and as north-south swaths, approximately 30° wide, of plains along meridians centered at the longitudes of Eastern Aphrodite (165°E, Atalanta, Rusalka, and Helen planitiae) and, 180° of arc away, at 345°E in Guinevere and Lavinia planitiae. Highlands are widely distributed and include Ishtar Terra, Aphrodite Terra, Tellus Regio, Alpha Regio, and Beta Regio.

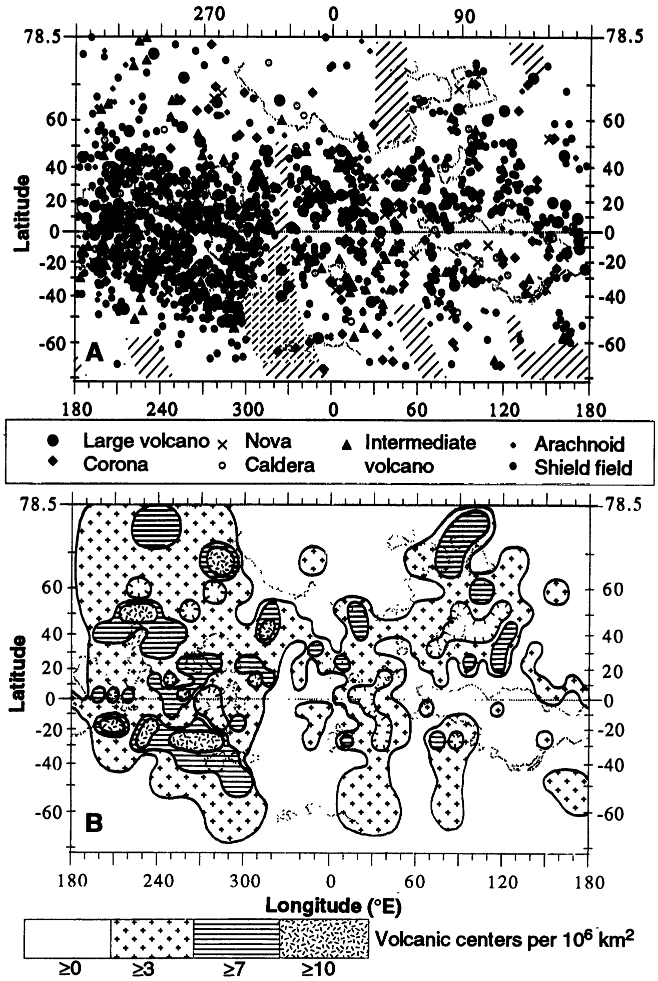

Fig. 1. (**A**) Mercator projection of the global distribution of volcanic and magmatic centers on Venus [from (*2, 3*)]. Dotted outlines indicate the main highland areas (regions >1 km above the mean planetary radius); ruled areas are not analyzed; the dashed rule indicates areas examined from Arecibo image data (*38*). The anomalously high concentration of volcanic centers in the western hemisphere occurs between the principal highland areas of Beta, Atla, and Themis regiones. For the location of regional feature names, see Fig. 3C. For definitions of the volcanic center types shown, see (*2, 3*). (**B**) Global contour map of volcanic center spatial density. All areas where spatial densities are in excess of the global mean are shaded. Note that the largest concentration is centered on the equator near longitude 250°E and is surrounded by regions of less than mean density. A more dispersed concentration occurs in the opposite hemisphere and is centered at approximately 70°E.

The relations of major concentrations of volcanism to regional geologic characteristics yield some information about the state of regional strain, modes of crustal deformation, and processes of crustal formation on Venus in general. We identified five types of widespread geological features on Venus of potential significance in this respect (*11*) and determined their distributions by preparing a series of maps based on global mosaicked image data (scale = 1:8,000,000) (Figs. 2A and 3, A and B). These features are fracture belts, ridge belts, mountain belts, ridged plains, and tesserae. On the basis of a comparison of the distribution of these geological characteristics and volcanic centers, the following general correlations and interpretations may be summarized (Fig. 4).

The largest contiguous area of fracture belts corresponds spatially with the area of the BAT anomaly (Fig. 2, A and B). Fracture belts are interpreted to be the sites of crustal extension and rifting, are globally abundant, and constitute a large fraction of the surface area in the low latitudes (±45°) between longitudes 190° and 320° (Fig. 2, A and B). Isolated, smaller areas of similar extensional characteristics occur in the opposite hemisphere. Because coronae are thought to develop from impingement of either deep mantle plumes (*12*) or shallow mantle instabilities on the overlying lithosphere, the similarity in location of the concentrations of coronae and the overall BAT anomaly implies that distributed mantle upwelling is plausibly associated with the main concentrations of volcanic centers and extensional deformation.

Volcanic centers are rare within tesserae (Fig. 3B), which include most of the highlands. Tesserae represent areas of complex fracturing and deformation, are usually the oldest local stratigraphic units (*13*), and appear to originate from complex, multiphase deformation involving extension and compression. The consistently higher surface elevation of tesserae and their associated gravity anomalies have been interpreted to reflect greater than average crustal thickness (*14*) and correspondingly different strength characteristics (*14, 15*). With the exception of a few small shield volcanoes, large volcanoes, and coronae, volcanism is absent within tesserae, even where such terrain occurs within the BAT anomaly (for example, Beta and Phoebe regiones). As tessera is generally the oldest local stratigraphic unit (*13*), it is unlikely to have deformed the latest volcanic centers. Some specific characteristic, such as rheological or altitude-induced differences in magma and country-rock density (*16*), appears likely to be responsible for impeding magma ascent in areas of tesserae.

Volcanic centers on Venus are also infrequent in areas characterized by ridge belts, mountain belts, and ridged plains. Ridge belts are common in the lowland plains of Lavinia, Atalanta, Rusalka, and Vinmara planitiae and are most frequent in the swath (30° wide) of meridional plains around the BAT anomaly at 165°E and 345°E. Mountain belts are restricted to Ishtar Terra. Both ridge belts and mountain belts (Fig. 3A) are interpreted to be the results of focused crustal shortening (*17*), differing primarily in the greater magnitude of inferred crustal shortening, higher topography, and orogenic belt character (*17*) of mountain belts. Ridged plains occur commonly in low and morphologically uniform plains (*18*) and in the high-latitude plains areas of Helen, Lavinia, and Aino planitiae in the southern hemisphere and Snegurochka and Atalanta planitiae in the northern hemisphere (Fig. 3A). They are characterized by uniformly oriented sinuous ridges across regions hundreds to thousands of kilometers in width (*18*) and are interpreted (*18*), by analogy with similar plains deformation styles observed elsewhere in the solar system (*19*), to represent areas of net regional crustal shortening in which individual ridges record crustal shortening of a few percent. Most of the lowland regions may be characterized geologically as broad plains consisting of vast sheets of lava and associated sinuous channels (*4*). Although the source vents cannot always be clearly identified, the distribution and ori-

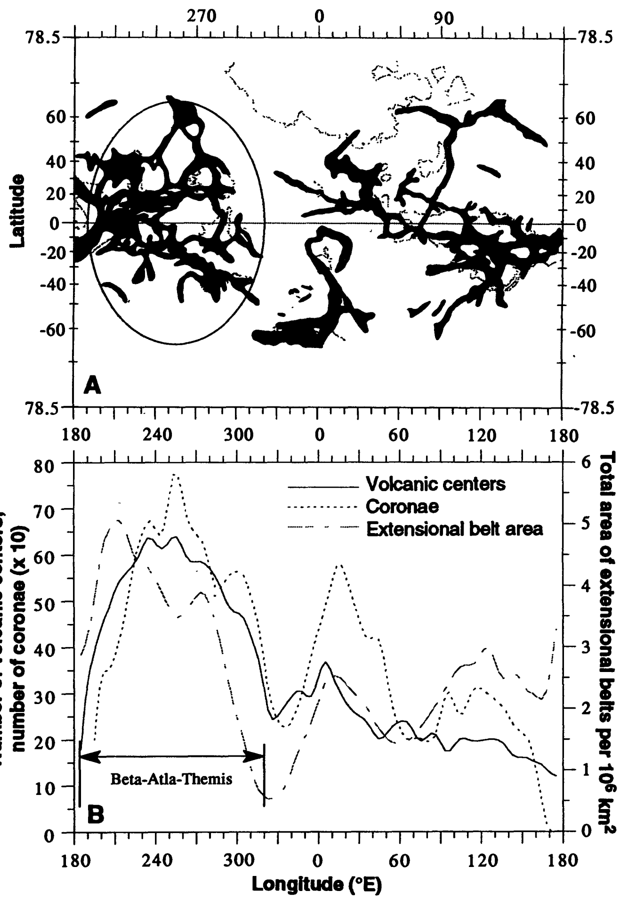

Fig. 2. (**A**) Global distribution of fracture belts (black) on Venus based on mapping from image data mosaicked at a scale of 1:8,000,000. The largest concentration of fracture belts occurs in the region between Beta, Atla, and Themis regiones. The circle is centered on the Beta, Atla, and Themis (BAT) concentration anomaly and is 130° in diameter. Fracture belts are interpreted to represent areas of enhanced crustal extension. (**B**) Correlation between the relative areas of fracture belts and the areal density of volcanic centers and coronae on Venus. Totals are determined for longitudinal bands 10° wide and ±45° in latitudinal extent. The greatest area of fracture belts coincides with the area over which volcanic centers occur with the greatest frequency (the BAT anomaly).

entation of distributary lava channels (*4*), flow fields (*2, 20*), and small shield volcanoes (*21*), all possible or presumed sources for plains lavas, imply that many of the observed lava floods originate near the uplands or from local volcanic edifices and flow toward the lowlands. Identification of large fissure-fed flows in the lowlands, if present, must await more detailed mapping.

The largest negative geoid anomalies occur in areas characterized by low volcanic center concentrations, such as Lavinia and Atalanta planitiae (Fig. 3C). Although the geoid on Venus is known to be strongly correlated with topography, the magnitude of the anomalies in many of these areas exceeds that attributable to topography alone (*22, 23*), and a dynamic downwelling component to the geoid signal is frequently inferred for most of the lowland areas (*23–25*) where the above observations indicate that there is abundant geological evidence for compressional deformation. There are additional means of generating the observed pattern of crustal shortening in the lowland plains, including far-field compressive stresses arising from the relatively static body forces associated with the largest regional rises (such as Aphrodite) (*18*). This mechanism was offered previously as an explanation of the similar annular arrangement of ridged plains on Mars about Tharsis

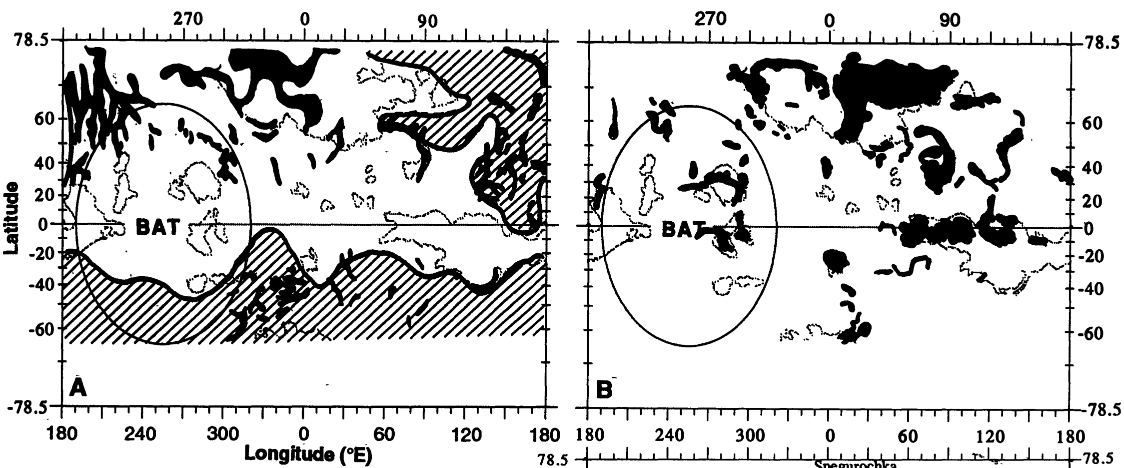

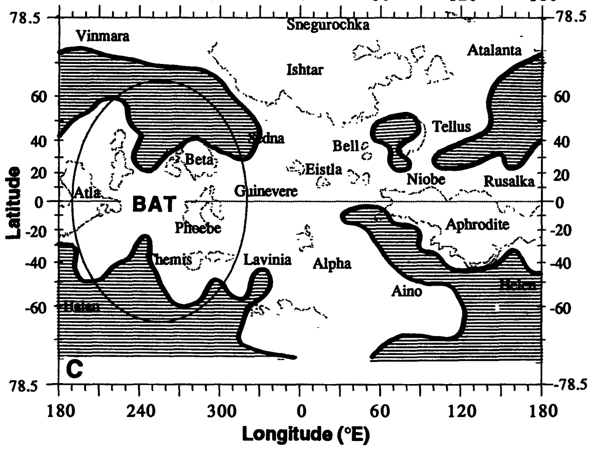

Fig. 3. (**A**) Global distribution of ridge belts and mountain belts (black) and ridged plains (diagonal ruled pattern) on Venus. All three of these geological features are interpreted to represent crustal shortening resulting from regional compressive stresses and occur with the greatest frequency outside the area of the BAT anomaly (circle). The extent of ridged plains is approximate. (**B**) Global distribution on Venus of tesserae, simplified from (*13*). (**C**) Distribution of anomalous (≤−20 m) geoid lows (indicated by ruled pattern). Based on an analysis of Pioneer-Venus data (*22*), a broad region containing geoid highs occurs in the location of the BAT anomaly and corresponds to a concentration of fracture belts and geological evidence for mantle upwelling. Compared to isolated geoid highs, geoid lows are more interconnected (*23, 28*) and occur generally within an annulus encompassing the BAT anomaly volcanic concentration.

(26). However, many of the inferred characteristics of strain predicted in association with convergence and downward flow of the mantle in the Venus environment (25) are consistent with the known elevation, distributed crustal shortening, and regional geoid anomalies seen in the lowlands and ridge belts. The regional downwelling of cool mantle and corresponding low regional heat flow throughout the lowlands and in areas characterized by ridge belts is consistent with infrequent melt generation and the paucity of volcanic centers in the lowlands.

On the basis of these large-scale, simple patterns of distribution of geological characteristics on Venus, their correlation with volcanism, and geological evidence for associated crustal extension and compression, we suggest that the pattern of mantle circulation on Venus might be relatively well organized at large scales: the BAT anomaly represents an area characterized by distributed mantle upwelling and is encircled by low plains characterized by compressional ridges and anomalous geoid lows that represent the effects of mantle downwelling (Fig. 4). Similar conclusions are based on an initial comparison of Magellan image and Pioneer-Venus gravity data (23). The abundance of large volcanic centers in the regions of extension and the relative dearth of volcanic centers in regions characterized by compression implies that positive and negative thermal or melting anomalies, respectively, are associated with these geological characteristics. Coronae on Venus need not represent plumes ascending from the deep mantle but might instead represent relatively shallow mantle instabilities that are enhanced regionally, as in the BAT anomaly, by broad-scale upwelling. Individually, they are not excluded from occurring in other dynamic settings. The current arrangement of large-scale surface geological characteristics on Venus may represent anomalous melting in broad areas, as represented by the BAT anomaly and as a result of geometrically simple, global (low harmonic degree and order) patterns of interior convection.

Large-scale thermal and chemical instabilities might originate by several means and suggest directions for future investigations. The mechanisms include normal cycles of fluid thermal convection (27, 28) or cyclical thermal convection styles (29, 30); forced convection arising from large-scale, possibly cyclical, boundary layer instabilities (30, 31); or intrinsic planetary-scale inhomogeneities in the mantle.

Recent studies have proposed that a massive resurfacing of Venus occurred about 500 million years ago, and several mechanisms have been postulated (9, 32) to account for the event. The patterns documented here may be linked to this event. For example, overturn of a negatively buoyant crust and depleted mantle layer or episodic plate tectonics may produce large-scale mantle convection patterns such as those observed (30, 31) that persist long after the initiating mechanism. In size and relative volcanic flux, the BAT anomaly might be comparable to short-lived "superplumes" (33) on Earth. More refined predictions of these models will permit these connections to be tested.

	Uplands	Lowlands	Highlands
2 km 0	0 to 2 km	<0 km	>2 km
Type areas	Beta-Atla-Themis (BAT) Eistla, Bell regiones	Guinevere, Lavinia, Rusalka, Vinmara, Helen, Atalanta planitiae	Ishtar, Aphrodite, Terra, Beta, Phoebe, Alpha, Tellus Regio
Volcanic centers	Abundant	Few	Few
Characteristics	Fractures Faults Troughs Rifts	Ridged plains Ridge belts Lava plains Lava channels/floods	Mountain belts Tessera terrain
Interpretation	Regional extension Rifting	Regional compression Reverse faulting Folding	Regional compression Folding Crustal thickening Shallow extension
Formation mechanism	Mantle upwelling	Mantle downwelling?	Regional upwelling? Global downwelling?

Fig. 4. Summary of the global altitude and geological setting of volcanic and magmatic anomalies on Venus and the geological interpretation and the inferred origin of each setting.

The observed arrangement between volcanic centers and tectonic features on Venus is consistent with recent three-dimensional modeling of large-scale convection in Earth's interior and the relation of that convection with tectonics and surface geology (27, 28, 34, 35). Numerical models of thermal convection in planetary interiors indicate that the pattern of convection for a wide range of rheological characteristics tends to organize into approximately equidimensional clusters of upwelling cells (27, 28) even though individual upwellings might originate from either shallow or deep instabilities, depending on the details of the forcing mechanism. However, one conclusion in current models is that the downwelling areas tend to be more organized and frequently form interconnected and approximately linear regions surrounding the more equidimensional areas of upwelling (28), which is in agreement with the geological evidence surrounding the BAT anomaly on Venus. The large, hemispheric size of the regions over which upwelling occurs implies a relatively deep mantle origin (28). The pattern of possible large-scale mantle motion on Venus that we have derived from the geological characteristics bears some similarity to the inferred large-scale structure of convection in the mantle of Earth. Two global concentrations of intraplate volcanic center abundances occur on Earth (7, 10, 34); these appear to be correlated with low density and warmer deep mantle anomalies, as determined from gravity and tomographic studies (28, 34), that are consistent with distributed upwelling, warming of the overlying mantle, and a correspondingly increased presence of partial melting in these areas relative to adjacent regions of the upper mantle (28). On Earth, the current, relatively simple pattern of distribution of subduction, the arrangement of continents and young orogenic belts, and the distribution of hot spots have been attributed to a fundamental, hemispherically symmetric large-scale structure of Earth's interior (34). Similar patterns appear to characterize the global geological arrangement of Venus.

Regardless of the mechanism or timing responsible for global-scale inhomogeneities in volcanic and tectonic features on Venus, these and other comparison studies (36) indicate that similar patterns appear to occur on the other terrestrial planets and differ only in the details of their manifestations and relative importance in their respective global tectonic settings. In this respect, the hemispheric volcanism concentration anomaly on Venus is comparable to patterns of intraplate volcanism on the other terrestrial planets, including Earth.

REFERENCES AND NOTES

1. R. S. Saunders *et al.*, *J. Geophys. Res.* **97**, 13067 (1992); R. S. Saunders *et al.*, *Eos* **73**, 178 (1992).
2. J. W. Head, *J. Geophys. Res.* **97**, 13153 (1992).
3. L. S. Crumpler, J. W. Head, J. C. Aubele, *Lunar Planet. Sci.* **XXIV**, 361 (1993).
4. V. R. Baker *et al.*, *J. Geophys. Res.* **97**, 13421 (1992); J. E. Guest *et al.*, *ibid.*, p. 15949.
5. B. Pavri, J. W. Head, K. B. Klose, L. Wilson, *ibid.*, p. 13445.
6. R. J. Phillips *et al.*, *ibid.*, p. 15923.
7. M. Stefanick and D. M. Jurdy, *ibid.* **89**, 9919 (1984).
8. This figure is based on the assumption that, in the absence of plate motions, hot spots on Earth would grow to dimensions comparable to those on Venus (>20 km).
9. G. G. Schaber *et al.*, *J. Geophys. Res.* **97**, 13257 (1992).
10. S. T. Crough and D. M. Jurdy, *Earth Planet. Sci. Lett.* **48**, 15 (1980); C. G. Chase, *Nature* **282**, 464 (1979).
11. Fracture belts and ridge belts, distinguished on the basis of evidence previously outlined from detailed studies of ridge belt occurrences in Lavinia Planitia (*25*), tend to occur as a system of linear, arcuate, and, in many cases, subparallel patterns of radar-bright lines. Ridge belts consist of numerous subparallel to anastomosing short and elongate (*37*) ridge-like forms and are frequently associated with regional linear to arcuate topographic swells. Ridged plains consist of numerous, subparallel and sinuous ridges like the "wrinkle" ridges common on the lunar mare and plains surfaces of Mars (*19*). Mountain belts occur in western Ishtar Terra and are mapped together with ridge belts.
12. E. R. Stofan *et al.*, *J. Geophys. Res.* **96**, 20933 (1991); E. R. Stofan *et al.*, *ibid.* **97**, 13347 (1992); S. W. Squyres *et al.*, *ibid.*, p. 13611; D. M. Janes *et al.*, *ibid.*, p. 16055.
13. M. A. Ivanov *et al.*, *Lunar Planet. Sci.* **XXIII**, 581 (1992); M. Ivanov and J. W. Head, *ibid.* **XXIV**, 691 (1993).
14. D. L. Bindschadler and J. W. Head, *J. Geophys. Res.* **96**, 5889 (1991); S. E. Smrekar and R. J.

Phillips, *Earth Planet. Sci. Lett.* **107**, 582 (1991).
15. S. C. Solomon *et al.*, *J. Geophys. Res.* **97**, 13199 (1992).
16. J. W. Head and L. Wilson, *ibid.*, p. 3877.
17. L. S. Crumpler *et al.*, *Geology* **14**, 1031 (1986); W. M. Kaula *et al.*, *J. Geophys. Res.* **97**, 16085 (1992); R. W. Vorder Bruegge and J. W. Head, *Geology* **19**, 885 (1991).
18. F. Bilotti and J. Suppe, *Geol. Soc. Am. Abstr. Progr.* **24**, A195 (1992); G. E. McGill, *Eos* **73**, 330 (1992).
19. T. R. Watters, *J. Geophys. Res.* **93**, 10236 (1988).
20. K. M. Roberts *et al.*, *ibid.* **97**, 15991 (1992).
21. J. C. Aubele and L. S. Crumpler, International Colloquium on Venus, *Lunar Planet. Inst. Contrib.* **789**, 7 (1992).
22. B. G. Bills *et al.*, *J. Geophys. Res.* **92**, 10335 (1987); R. J. Phillips and M. C. Malin, in *Venus*, D. M. Hunten *et al.*, Eds. (Univ. of Arizona Press, Tucson, 1984), pp. 159–214.
23. R. R. Herrick and R. J. Phillips, *J. Geophys. Res.* **97**, 16017 (1992).
24. D. L. Bindschadler *et al.*, *ibid.*, p. 13495; D. L. Bindschadler and E. M. Parmentier, *ibid.* **95**, 21329 (1990).
25. S. W. Squyres *et al.*, *ibid.* **97**, 13579 (1992); R. J. Phillips, R. E. Grimm, M. C. Malin, *Science* **252**, 651 (1991); M. T. Zuber, *Geophys. Res. Lett.* **17**, 1369 (1990).
26. W. B. Banerdt *et al.*, *J. Geophys. Res.* **87**, 9723 (1982).
27. G. Schubert *et al.*, *ibid.* **95**, 14105 (1990).
28. D. Bercovici, G. Schubert, G. A. Glatzmaier, *Science* **244**, 950 (1989); D. Bercovici *et al.*, *Geophys. Res. Lett.* **16**, 617 (1989); P. Olson, P. G. Silver, R. W. Carlson, *Nature* **344**, 209 (1990); A. V. Malevsky *et al.*, *Geophys. Res. Lett.* **19**, 127 (1992).
29. J. Arkani-Hamed and N. Toksoz, *Phys. Earth Planet. Inter.* **34**, 232 (1984); D. L. Anderson, *Nature* **297**, 391 (1982).
30. D. L. Turcotte, *Eos* **73**, 329 (1992).
31. E. M. Parmentier and P. Hess, *Geophys. Res. Lett.* **19**, 2015 (1992).
32. S. C. Solomon, *Lunar Planet. Sci.* **XXIV**, 1331 (1993).
33. R. L. Larson, *Geology* **19**, 547 (1991).
34. A. Cazenave, A. Souriau, K. Dominh, *Nature* **340**, 54 (1989); M. A. Richards *et al.*, *J. Geophys. Res.* **93**, 7690 (1988).
35. C. Vigney, Y. Ricard, C. Froidevaux, *Tectonophysics* **187**, 345 (1991); Y. Ricard and C. Vigney, *J. Geophys. Res.* **94**, 17543 (1989); M. Gurnis, *Nature* **332**, 695 (1988).
36. L. S. Crumpler *et al.*, *Lunar Planet. Sci.* **XXIV**, 359 (1993).
37. V. L. Barsukov *et al.*, *J. Geophys. Res.* **91** (suppl.), D378 (1986).
38. D. B. Campbell, D. A. Senske, J. W. Head, A. A. Hine, P. C. Fisher, *Science* **251**, 180 (1991); D. A. Senske *et al.*, *Earth Moon Planets* **55**, 97 (1991).
39. This analysis was carried out under funding from the NASA Magellan Project.

1 March 1993; accepted 3 June 1993

Detection of a Meteoritic Component in Ivory Coast Tektites with Rhenium-Osmium Isotopes

Christian Koeberl and Steven B. Shirey

Measurement of rhenium (Re) and osmium (Os) concentrations and Os isotopic compositions in Ivory Coast tektites (natural glasses with upper crustal compositions that are ejected great distances during meteorite impact) and rocks from the inferred source crater, Lake Bosumtwi, Ghana, show that these tektites incorporate about 0.6 percent of a meteoritic component. Analysis of elemental abundances of noble metals alone gives equivocal results in the detection of meteoritic components because the target rocks already have relatively large amounts of noble metals. The Re-Os system is ideally suited for the study of meteorite impacts on old continental crust for three reasons. (i) The isotopic compositions of the target rocks and the meteoritic impactor are significantly different. (ii) Closed-system mixing of target rocks and meteorites is linear on Re-Os isochron diagrams, which thus permits identification of the loss of Re or Os. (iii) Osmium isotopic compositions are not likely to be altered during meteorite impact even if Re and Os are lost.

Tektites are natural glasses occurring on Earth in four distinct areas known as strewn fields: the Australasian, Ivory Coast, Central European, and North American fields (*1, 2*). Tektites occur in various forms on land (*1, 2*) and as microtektites (generally <1 mm in diameter) in deep-sea cores. Geochemical data show that tektites have been derived from terrestrial upper crustal rocks by melting caused by hypervelocity impact (*1–4*). Although a meteoritic component has been reported for impact glasses, melts, and breccias at several impact craters (*5*) and meteorite (projectile) compositions have been estimated (*6, 7*), unequivocal identification of an extraterrestrial component has not been made for tektites (*2*). Tektites consist predominantly of terrestrial material (*4*) because the meteoritic projectile is vaporized on impact (*8*). The only elements that seem to be diagnostic of a meteoritic component are some siderophile elements, especially members of the platinum group elements (PGEs). Their abundances and interelement ratios in meteorites are considerably different from those in terrestrial crustal rocks. By using the Re-Os isotopic system, we are trying to characterize the isotopic differences between the source rocks and the tektites and learn more about the impact process. Here, we present Re-Os isotopic analyses of Ivory Coast tektites that show the presence of a meteoritic component (not exceeding 0.6%). This result supports the link between the tektites and their presumed source crater and suggests Re and Os loss during the impact process.

C. Koeberl, Institute of Geochemistry, University of Vienna, Dr.-Karl-Lueger-Ring 1, A-1010 Vienna, Austria, and Department of Terrestrial Magnetism, Carnegie Institution of Washington, 5241 Broad Branch Road NW, Washington, DC 20015.
S. B. Shirey, Department of Terrestrial Magnetism, Carnegie Institution of Washington, 5241 Broad Branch Road NW, Washington, DC 20015.

The abundance of PGEs is low in tektites and, as a result, only few tektites have been analyzed for their PGE contents. Morgan (*9*) analyzed six high-Mg australites by radiochemical neutron activation analysis; only one showed a distinct PGE enrichment over the typical abundances in upper crustal rocks, but the data did not allow the characterization of the projectile. Palme and co-workers (*7, 10*) analyzed the PGE content of two Ivory Coast tektites. Abundances of Ir and Os were 0.24 and 0.33 ppb and 0.099 and 0.199 ppb, respectively; the abundances of all other PGEs were below detection limits. Palme *et al.* (*10*) suspected that an iron projectile might have been responsible for the Bosumtwi crater, but Jones (*11*) argued that the target rocks could supply the high Ir content because the Bosumtwi crater is in an area of gold mineralization. Thus, the available data were insufficient to definitely identify the meteorite group of the projectile or its contribution to the tektites. The problem of identification is amplified by unpredictable fractionation between individual PGEs and other siderophile elements during impact (*12, 13*).

Here, we show that the Re-Os isotopic system can be used to quantify target-bolide mixing during impact and to understand better the impact process. Osmium isotopes are able to provide an unambiguous tracer for the presence and proportion of an extraterrestrial component in tektites, impact glasses, and other impact-derived rocks and may help identify the target material. The absolute abundance of Os (and other PGEs) as well as the ratios of $^{187}Re/^{188}Os$ and $^{187}Os/^{188}Os$ in meteorites are distinctly different from the values obtained for old continental crustal rocks that make up the target material for tektites. It is unlikely that there is a significant fractionation of Os isotopes during impact. In an earlier study, Fehn *et al.* (*14*) determined Os isotopes in suevite and impact melts from the Ries and East Clearwater craters; however, the analytical methods were not yet sensitive enough to allow a quantitative discussion of any meteoritic contamination.

The Re-Os isotopic system has important implications for the study of the mantle-crust system (*15*) and meteorite chronology (*16–18*). It is based on the decay of